Springer

KSME

Journal of Mechanical Science and Technology 26 (9) (2012) 2949~2958
www.springerlink.com/content/1738-494x
DOI 10.1007/s12206-012-0702-2

CFD analysis of fin tube heat exchanger with a pair of delta winglet vortex generators †

Seong Won Hwang[1], Dong Hwan Kim[1], June Kee Min[2] and Ji Hwan Jeong[1,*]

[1]*School of Mechanical Engineering, Pusan National University ,30 Jangjeon-Dong, Geumjeong-Gu, Busan 609-735, Korea*
[2]*Rolls-Royce University Technology Center, Pusan National University, 30 Jangjeon-Dong, Geumjeong-Gu, Busan 609-735, Korea*

(Manuscript Received June 19, 2011; Revised March 29, 2012; Accepted April 16, 2012)

Abstract

Among tubular heat exchangers, fin-tube types are the most widely used in refrigeration and air-conditioning equipment. Efforts to enhance the performance of these heat exchangers included variations in the fin shape from a plain fin to a slit and louver type. In the context of heat transfer augmentation, the performance of vortex generators has also been investigated. Delta winglet vortex generators have recently attracted research interest, partly due to experimental data showing that their addition to fin-tube heat exchangers considerably reduces pressure loss at heat transfer capacity of nearly the same level. The efficiency of the delta winglet vortex generators widely varies depending on their size and shape, as well as the locations where they are implemented. In this paper, the flow field around delta winglet vortex generators in a common flow up arrangement was analyzed in terms of flow characteristics and heat transfer using computational fluid dynamics methods. Flow mixing due to vortices and delayed separation due to acceleration influence the overall fin performance. The fin with delta winglet vortex generators exhibited a pressure loss lower than that of a plain fin, and the heat transfer performance was enhanced at high air velocity or Reynolds number.

Keywords: Fin-tube heat exchanger; Plate and fin tube; Delta winglet; Vortex generators; Flow separation

1. Introduction

Generally used to exchange heat between a gas and liquid, fin-tube heat exchangers are widely used in chemical processing plants, power plants, and home appliances, including small air conditioners and refrigerators [1]. While early fin-tube heat exchangers primarily adopted plain fins, extensive research on fin shape caused substantial progress in the development of high performance fins to produce compact heat exchangers. Current compact fin-tube heat exchangers adopt a slit or louver fin if the working fluid is not significantly corrosive, such as in the case of a fume gas.

Fin shapes for compact heat exchanger design are continuously studied to address related global environmental concerns and improve the efficiency of the energy system. One notable subject is the incorporation of vortex generators in fins. Early vortex generator research focused on the boundary layer control of air foils [2]. Vortex generators create longitudinal vortices in the main flow to re-energize the boundary layer that is developed adjacent to an air foil and, in turn, delay or prevent flow separation. The flow mixing caused by vortices enhances heat transfer, and thus researchers became interested in applying vortex generators to heat exchanger fin designs. The shape of existing vortex generators includes a rectangular wing, rectangular winglet, delta wing, and delta winglet. Recent research on the effects of vortex generators on the performance of fin-tube heat exchangers focused on delta winglet vortex generators (DWVG) rather than on other shapes.

The vortex generators incorporated in fin-tube heat exchangers can be categorized based on their configurations with respect to heat transfer tubes, whether 'common flow down' and 'common flow up', as illustrated in Fig. 1. The common flow down configuration has a pair of vortex generators mounted behind a tube (at the downstream). Fiebig [3] contended that this configuration would delay flow separation and reduce drag. In the common flow up configuration, a pair of vortex generators is installed in front of the tube (at the upstream). Torii et al. [4] speculated that this configuration accelerates the flow between a tube and its vortex generators as well as delays flow separation; thereby reducing the wake region behind the tube.

The effects of vortex generators on the performance of the heat transfer surface have been investigated in recent decades.

*Corresponding author. Tel.: +82 51 510 3050, Fax.: +82 51 515 4038
E-mail address: jihwan@pusan.ac.kr
† Recommended by Associate Editor Man-Yeong Ha

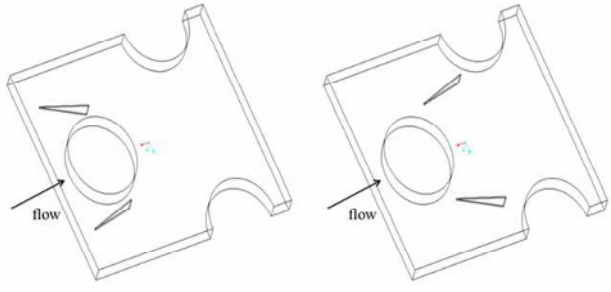

Fig. 1. Vortex generator configuration: (a) common flow up; (b) common flow down.

Jacobi and Shah [5] reviewed previous works until the early 1990s. They explained physical phenomena and vortex characteristics associated with vortex generators on a fin as well as introduced experiments and analysis on the performance of heat exchangers with vortex generators. They categorized active and passive methods of vortex generation. Active methods generate vortices using external energy, such as electric or acoustic fields, mechanical device, or surface vibration. Passive methods generate vortices through structures and additional fluids. Regardless of method, vortex generators enhance heat transfer and simultaneous pressure drop due to form loss. The vortex generator has the interesting characteristic of having a small pressure loss compared with other interrupted fin designs. As such, most previous works focused on quantifying the improvement of heat transfer performance and additional pressure drop characteristics.

Fiebig et al. [6] experimentally studied heat transfer performance in a channel with vortex generators in a common flow down configuration. The DWVG increases convective heat transfer by developing a boundary layer, swirl, or vortices, as well as through flow destabilization or turbulence intensification. The delta winglet enhances heat transfer more than a rectangular winglet. The highest heat transfer coefficient was obtained at a 45° attack angle, which is defined as the angle between the flow direction and vortex generators. The effects of the vortex generators on fin-tube heat exchangers were similarly experimentally investigated. The DWVG were installed onto 3-row fin-tube heat exchangers in a common flow down configuration. The staggered and inline effects of tube arrays on the thermal-hydraulic performance of the DWVG were compared. At nearly the same heat transfer coefficient, t he f-factor of the staggered array was smaller than that of the inline array in a range of $Re > 1300$. The DWVG can reduce the size and mass of a heat exchanger for a given heat load.

Kwak et al. [7] measured the heat transfer coefficient and pressure drop in 2, 3, 4, and 5-row fin-tube heat exchangers with a common flow up configuration DWVG in a range of $280 < Re < 2400$. The DWVG were only mounted on the first row. Compared with heat exchangers with plain fins, those with DWVG fins showed a 10% increase in heat transfer performance of the j-factor for all heat exchangers, and a 0%–10% increase of the f-factor for the 2, 4, and 5-row heat exchangers. For the 3-row heat exchanger, however, the f-factor dramatically decreased by 30%–50%. This was attributed to the effects of vortices, which were produced at the first row of the tube but did not reach the fourth and fifth rows.

Kwak et al. [8] investigated the effect of the number of DWVG rows, as well as measured the heat transfer capacity and pressure drop of staggered array fin-tube heat exchangers that were identical except for the number of DWVG rows. The heat exchanger with a single DWVG row experienced 10%–30% larger heat transfer capacity and 34%–55% less pressure drop than the heat exchanger without the DWVG. For the heat exchanger with two DWVG rows, however, heat transfer capacity and the pressure drop increased by 6%–15% and by 61%–117%, respectively, compared with the heat exchanger with a single DWVG row. The DWVG in the second row obstructed and decelerated the air flow to produce an additional pressure drop.

Recently, Joardar and Jacobi [9] investigated the effect of the number of DWVG rows in the inline array fin-tube heat exchangers. Single and three DWVG fin tube heat exchangers were compared with a plain fin tube heat exchanger. The DWVG was placed in a common flow up configuration. For the single DWVG, the heat transfer coefficient was enhanced by 16.5%–44% as pressure drop increased by less than 12%. For the case of three DWVG rows, the heat transfer coefficient was augmented by 29.9%–68.8% as the pressure drop penalty increased 26% at $Re = 960$ and 87.5% at $Re = 220$. DWVG arrays can significantly enhance the performance of fin tube heat exchangers with flow depths and fin densities typical of those used in air-cooling and refrigeration applications.

Allison and Dally [10] similarly examined the performance of the DWVG in flat fin tube heat exchangers, and compared the performance of two fin types. The first is a plain fin with a DWVG and the second is a louvered fin. The DWVG were installed in a common flow up configuration. The j- and f-factors of the heat exchanger with the DWVG were 87% and 53%, respectively, of the heat exchangers with a louver fin. Researchers also investigated the performance of DWVG fins through numerical analyses.

Min and Xu [11] numerically evaluated and compared the performances of a plain, DWVG, and louver fins incorporated in a flat tube heat exchanger. When compared with the heat exchanger with a plain fin, that with a louver fin had a heat transfer capacity of about 114.1%–139.1% with a pressure drop penalty of 163.9%–171.7%. In the case of the DWVG fin heat exchangers, heat transfer capacity was about 46.5%–74.1% and the pressure drop was 46.1%–49.7%. The significant variation in pressure drop could be attributed to the louver fin undergoing flow decay at each slit, whereas the winglet fin had no flow decay.

The above brief review shows that previous research mainly focused on the quantitative and qualitative effects of vortex generators on pressure drop and heat transfer performance,

through either experimental or numerical approach. Vortex generators were verified to enhance heat transfer. However, the pressure drop penalty was less consistent, reflecting a lack of phenomenological understanding of how vortex generators influence the heat transfer performance and pressure drop, because few research investigated this underlying mechanism. Thus, the present work aims to deepen the understanding on the DWVG enhancement of heat transfer performance with a relatively small, or even reduced, pressure drop penalty. Information on the fluid flow and heat transfer in a fin-tube heat exchanger with DWVG was obtained through computational fluid dynamics (CFD).

2. Numerical modeling and analysis

In the present work, steady-state Reynolds Averaged Navier-Stokes (RANS) equations were numerically solved for the coolant flow inside the reactor pool. Three-dimensional continuity and momentum conservation equations can be written as follows:

Mass conservation equation

$$\frac{\partial}{\partial x_i}(\rho u_i) = 0 \tag{1}$$

Momentum conservation equation

$$\frac{\partial}{\partial t}(\rho u_i u_j) = -\frac{\partial p}{\partial x} + \frac{\partial}{\partial x_i}\left[\mu\left(\frac{\partial u_i}{\partial x_j} + \frac{\partial u_j}{\partial x_i}\right) - (\rho\overline{u_i u_j})\right] \tag{2}$$

Energy conservation equation

$$\frac{\partial}{\partial x}(\rho C_p T u_i) = -\frac{\partial}{\partial x_i}\left(-k\frac{\partial T}{\partial x_i} + \rho C_p \overline{u_i' T'}\right) \tag{3}$$

where u, ρ, t, p, μ, T, k, and C_p represent the velocity, density, time, pressure, dynamic viscosity, temperature, thermal conductivity, and constant-pressure specific heat, respectively. Air flow passing around a circular tube will be influenced by various factors. When flow velocity is extremely low (Re << 1), the flow is dominantly affected by the inertial force and maintains a normal stream at the back of the tube. In a range of Re < 50, rather than the inertial force, the viscous force of the fluid prevails on the air flow. An adverse pressure gradient may thus develop, leading to a flow separation from the tube that no longer has a smoothly changing stream line. When flow separation occurs, a wake develops in the rear of the tube where the flow swirls and does not mix with external flow. This wake is usually detrimental in terms of heat transfer capacity and pressure loss [12].

Fig. 2 shows the representative geometry of a two-row fin-tube heat exchanger considered for the numerical analysis Delta winglet vortex generators are installed around the first row of the tube in a common flow up configuration. Notations

Table 1. Heat exchanger geometric data.

Notation	Meaning	Value
L	Length (m)	0.0254
W	Width (m)	0.021
D	Tube diameter (m)	0.008
t_{th}	Fin thickness (m)	0.0015
H	Fin pitch (m)	0.00123
Wl	Winglet length (m)	0.00565
Wh	Winglet height (m)	0.011
a	Attack angle (°)	15
b	Central angle (°)	110
g	Distance between tube and winglet (m)	0.001

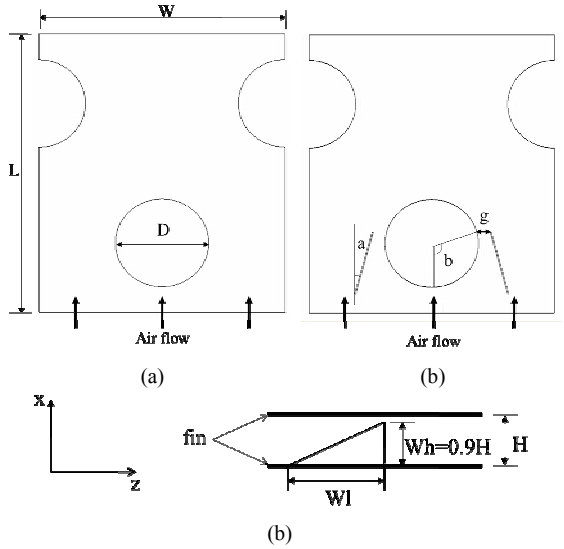

Fig. 2. Geometry definitions: (a) Plain fin-tube heat exchanger; (b) DWVG fin-tube heat exchanger; (c) DWVG.

for geometric definitions are also provided in Fig. 2. Table 1 lists the geometric values. Fin thickness, fin spacing, and tube size are similar to those of fin-tube heat exchangers that are widely used in condensers and evaporators of air-conditioners. The geometry and installed location of the delta winglet vortex generators are similar to those applied in the heat exchanger experimentally investigated by Kwak et al. [7]. Conjugate heat transfer was analyzed. Fig. 3 shows the solid domain mesh of the DWVG fin-tube heat exchanger. A cylindrical ring represents the heat transfer tube and a flat plate represents the fin. The triangular structure on the flat plate is the DWVG. Above the meshes for the solid part are those for the fluid part. Fine meshes are generated in the vicinity of the solid surface where the velocity gradient is large. The mesh size increases with the distance from the solid surface. The grid size was determined by testing three different fluid meshes: 4.5 million; 2.3 million; and 1.1 million.

The results of 4.5 million and 2.3 million meshes were consistent, whereas that of the 1.1 million meshes deviated by over 10%. Finally, 2.3 million meshes in total for the fluid

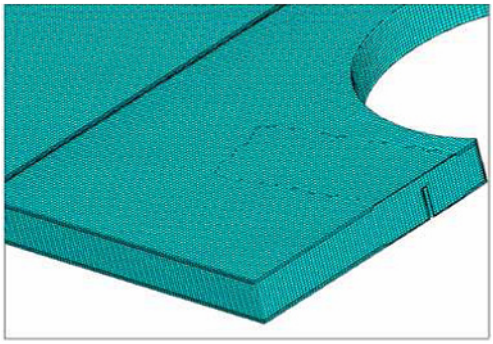

(a)

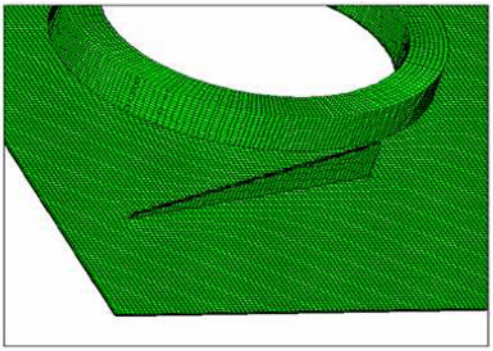

(b)

Fig. 3. Mesh configuration: (a) fluid mesh; (b) solid mesh.

domain and 0.4 million meshes for the solid part were used for the present computations. Figs. 3(a) and (b) show the meshes. The semi-implicit method for pressure-linked equations (SIMPLE) algorithm [13] is used.

Air flow is assumed incompressible and turbulent. RNG k-ε model was used as a turbulence model, considering complex flows (wake or separation) and anisotropic turbulence. The boundary conditions are as follows. An inlet velocity boundary condition (0.5–20 m/s) is established for the front end of the fluid domain, whereas an outlet boundary condition is used for the rear end. Symmetric boundary condition is specified at both side-ends of the flow path. A constant temperature condition was set at the inner tube wall. The temperature of the solid surface was set such that the heat flux through the solid part balances with that through the adjacent air. Top and bottom surfaces were set to adiabatic. The air inlet temperature was fixed at 293 K for all simulations. The heat transfer tube inner wall temperature was set at 333 K to represent a working condition of a refrigerant condenser.

The following expressions analyzed the data. The heat transfer coefficient is related with the temperature difference, as follows:

$$Q = \dot{m} c_p \left| T_{in} - T_{out} \right| \tag{4}$$

$$h = \frac{Q}{(A_c + A_{fin}) \Delta T_{LM}} \tag{5}$$

$$\Delta T_{LM} = \frac{(T_c - T_{in}) - (T_c - T_{out})}{\ln \left| \frac{T_c - T_{in}}{T_c - T_{out}} \right|} \tag{6}$$

where $\dot{m}$, A_c, A_{fin}, T_{in}, T_{out}, T_c, and Q represent the mass flow rate, fin collar area, fin surface area, maximum velocity, inlet air temperature, outlet air mean temperature, fin collar temperature, and total heat transfer rate, respectively. T_{in} is constant because we set it as a boundary condition at the entrance. However, T_{out} varies over the cross-sectional plane at the exit because it is influenced by heat transfer and fluid flow. An area average value was used in this work and is given as follows:

$$T_{out} = \frac{\int |u| T dA_f}{\int |u| dA_f} \tag{7}$$

where A_f represents the fluid cross sectional area at the exit. The thermodynamic properties in the above equations are typically temperature dependent. Application of the above equations to temperature-varying situations use the average values of properties evaluated at the lowest and the highest temperatures. Based on the CFD results, the average convective heat transfer coefficient can be obtained using the relationships of Eqs. (4)-(7). Substituting this coefficient value for Eqs. (8) and (9) can obtain the f-factor and the Colburn-j factor. The friction factor is given as follows:

$$f = \frac{\Delta \mathrm{P}}{(\rho \times \mathrm{V}_{\max}^2 / 2)} \left(\frac{D_c}{4L} \right) \tag{8}$$

where ΔP and D_c represent the pressure difference and characteristic length, respectively. The diameter of the fin collar is used. V_{max} represent the maximum velocity, which is the average velocity at the minimum cross sectional area (A_{min}) in flow direction, defined as $U(A_f / A_{min})$

$$\frac{C_f}{2} = \frac{Nu_x}{\mathrm{Re}_x \mathrm{Pr}} \times \mathrm{Pr}^{2/3} = St_x \mathrm{Pr}^{2/3} \equiv j \tag{9}$$

where St represents the Stanton number and j is the Colburn j-factor. This relationship is called the Reynolds-Colburn analogy, and implies that the heat transfer performance is enhanced with an increase in the frictional pressure drop [14]. Heat transfer augmentation with a minimum pressure drop increase is preferred in enhanced heat transfer surface designs [15].

At the beginning of the CFD analyses, a preliminary calculation determined whether the air flow shows any transient behavior. A fluid flowing around a tube may cause vortex shedding, which is known as the Strouhal number defined by Eq. (10) to be 0.2 [16].

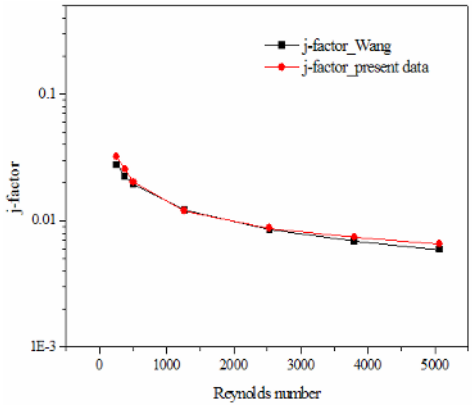

Fig. 4. Validation result with Wang et al.'s [17] correlation.

$$S = \frac{f_v D}{u} \tag{10}$$

where S, f_v, and D represent the Strouhal number, vortex shedding frequency, and tube diameter, respectively. The vortex shedding frequency may then be obtained by substituting the values of S, u, and D into Eq. (10). A transient simulation was performed for two period times, but no vortex shedding was observed. Thus, subsequent calculations only determined the values for the steady state.

Fig. 4 shows the j-factor of the plain fin-tube heat exchanger evaluated by the CFD analysis, which coincides with that estimated by the empirical correlation of Wang et al. [17].

This comparison proves that the present numerical models are appropriate.

3. Numerical result

Fig. 5 shows the air flow velocity vector at the mid-plane between two fins when the frontal air velocity is 5 m/s. The air enters from the left-hand side and flows around the heat transfer tube. The air flow then separates from the tube wall and develops a wake region behind the tube, and enters the fin-tube heat exchanger where the flow slows down and circulates [14]. For a plain fin heat exchanger, as seen in Fig. 5(a), the wake is wide and extends to the tailing edge of the fin. For a DWVG fin, as seen in Fig. 5(b), the flow velocity increases between the DWVG and the heat transfer tube. Then the flow separation point moves to the rear side of the tube, where in this case, a narrower and shorter wake region still develops. The wake region appears to be extended lengthwise to the middle of the second row of tubes. Fig. 5(b) shows that the air flow accelerates between the DWVG and tube wall, consequently forming a delayed, adverse pressure gradient. Furthermore, the flow separation occurs further downstream. This delayed flow separation diminishes the wake region and increases the uniformity of the overall velocity profile.

Fig. 6 shows the velocity vector plots of the frontal section. The DWVG creates the vortex. In Fig. 6(b), the vortex is generated in counter-clockwise at the left of the DWVG. At the same time, a secondary vortex flows at the upper vortex between the DWVG and the right side wall. These two vortex flows combine and form one counter-clockwise vortex at the end part of the DWVG as the separation wall disappears. This vortex flow develops at the rear, and thus, influences separation delays and reduces drag across the tube. Finally, the flow removes the poor heat transfer zone from the wake zone of the tube [4]. Moreover, the vortex mixes the flow, which improves convective heat transfer.

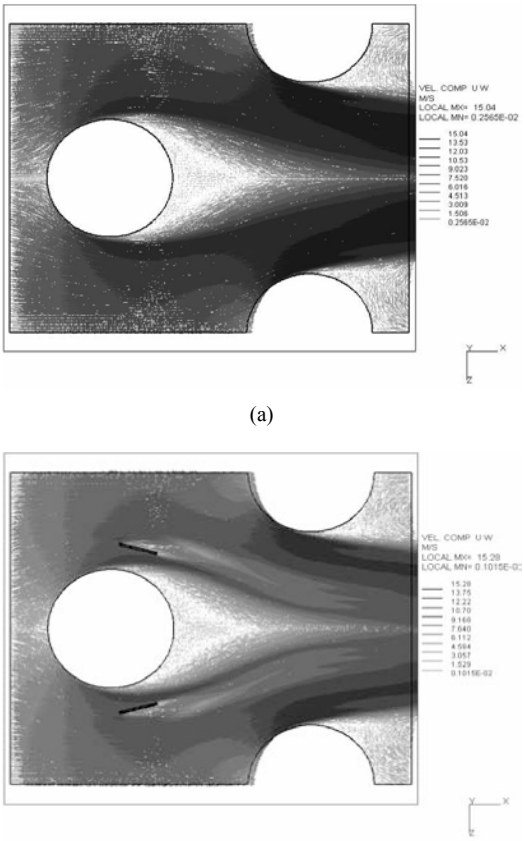

(a)

(b)

Fig. 5. Velocity vector of air at mid-plane (Re = 1295, Vmax = 8.07 m/s): (a) Plain fin-tube heat exchanger; (b) DWVG.

Fig. 7 shows the static pressure contour for the same case. The arrows indicate the adverse pressure gradient points where the pressure on the cylinder wall is at minimum. Th is point mainly affects the location of flow separation in the downstream. The static pressure at the tube wall decreases from the fore-end of the tube to the arrowhead. However, static pressure recovers at positions further on the rear. Fig. 7 shows that the DWVG influences the adverse pressure gradient point, which occurs at around 94.6° for the plain fin and at around 100.4° for the DWVG fin from the tube fore-end. This change in the adverse pressure gradient point influences the variation of the wake region, as shown in Fig. 5.

Fig. 8 shows the static pressure distribution at the mid-plane between two adjacent fins when the frontal air velocity is 15

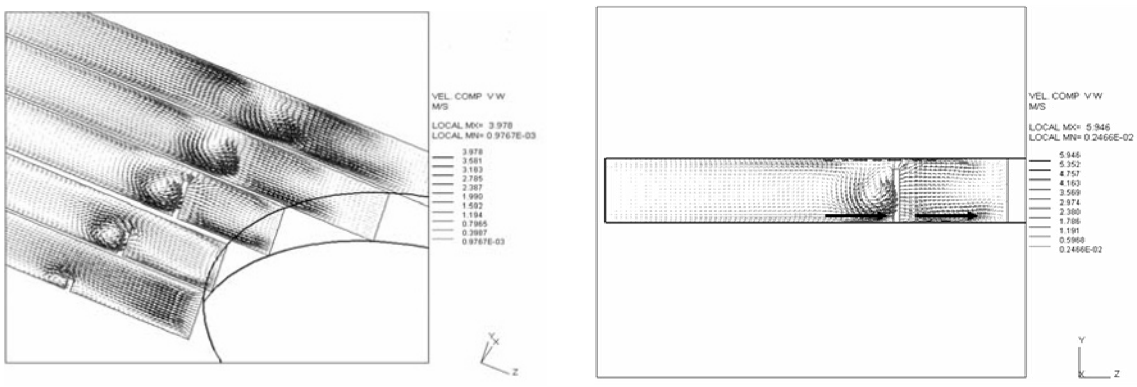

(a) (b)

Fig. 6. Velocity vector plot of vertical section (Re = 1295, V_{max} = 8.07 m/s): (a) velocity vector plots nearby tube; (b) velocity vector plot on a cross section with the DWVG.

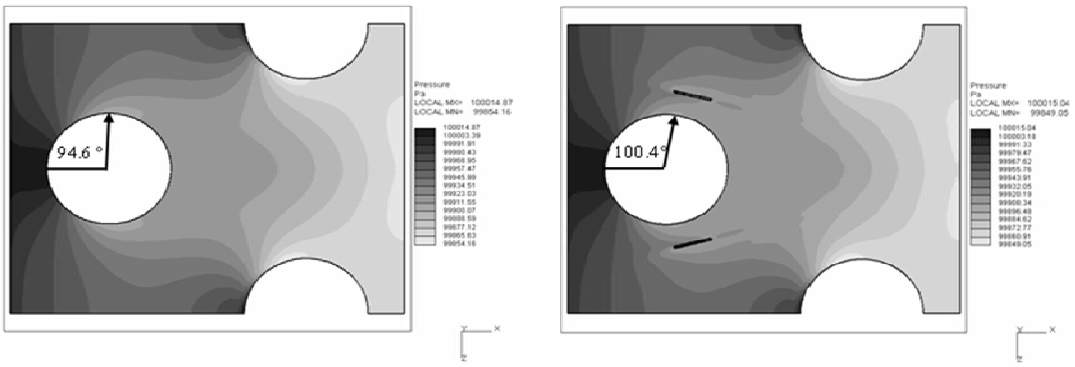

(a) (b)

Fig. 7. Static pressure contour at mid-plane and the adverse pressure gradient point on the cylinder (Re = 1295, V_{max} = 8.07 m/s): (a) Plain fin tube heat exchanger; (b) DWVG fin tube heat exchanger.

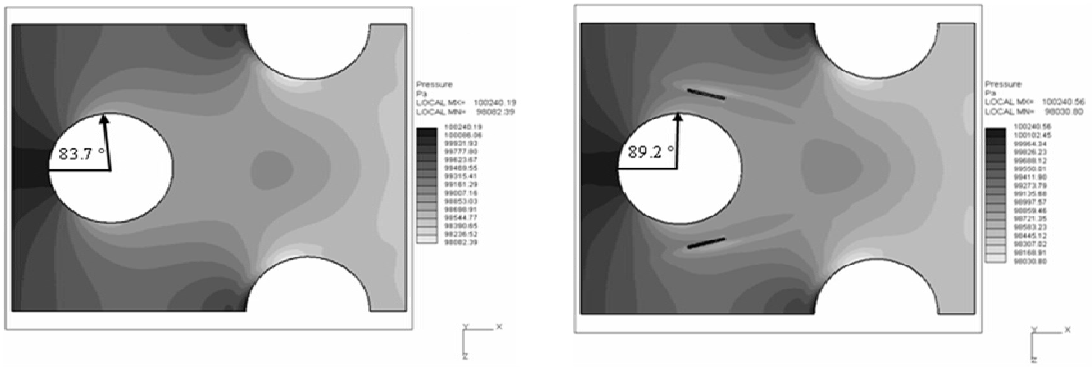

(a) (b)

Fig. 8. Static pressure contour at mid-plane and the adverse pressure gradient point on the cylinder (Re = 5180, V_{max} = 32.3 m/s): (a) Plain fin tube heat exchanger; (b) DWVG fin tube heat exchanger.

m/s. Fig. 8(a) shows the case of the plain fin, where the adverse pressure gradient point shifted to the front compared with that for a frontal air velocity of 5 m/s. The wake region thus widened and elongated. Fig. 8(b) shows the case of a DWVG fin, where the adverse pressure gradient point similarly occurs at a smaller angle compared with that of air velocity at 5 m/s depicted in Fig. 7(b). However, the size of wake region is smaller than that of the plain fin, proving that the effect of DWVG is still advantageous.

Fig. 9 shows the temperature distribution of air when its

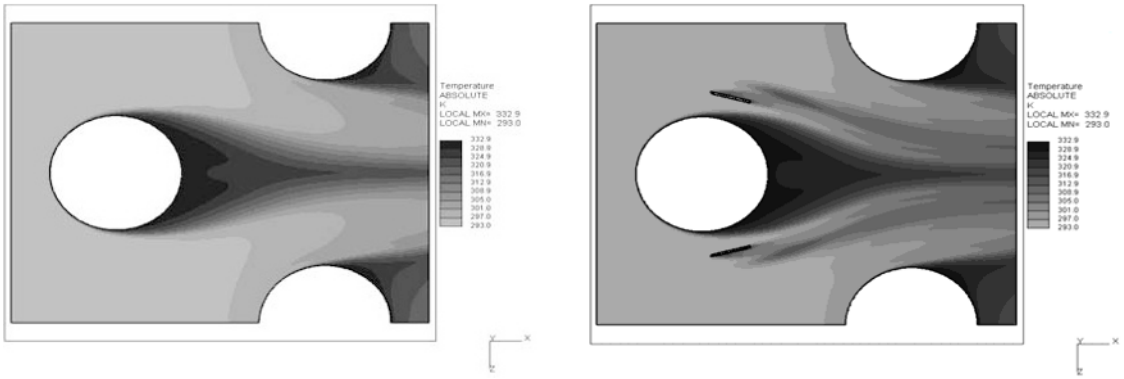

(a) (b)

Fig. 9. Air temperature at mid-plane (Re = 1295, V_{max} = 8.07 m/s): (a) Plain fin tube heat exchanger; (b) DWVG fin tube heat exchanger.

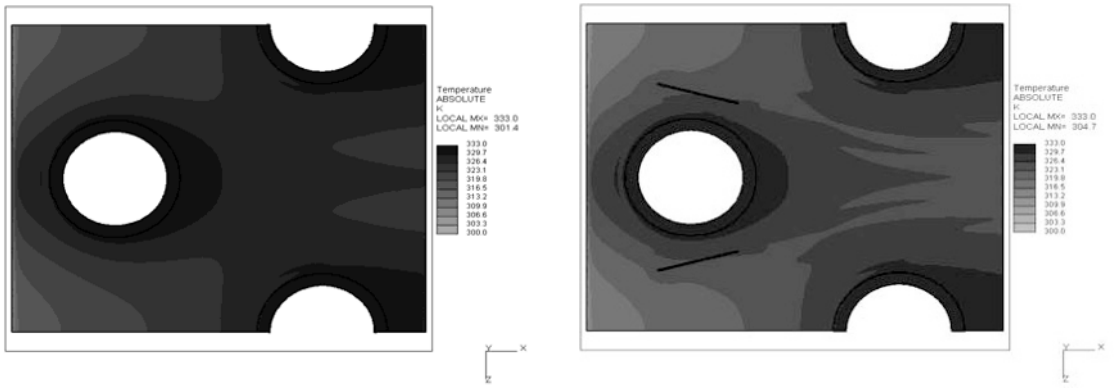

(a) (b)

Fig. 10. Fin surface temperature (Re = 1295, V_{max} = 8.07 m/s): (a) Plain fin tube heat exchanger; (b) DWVG fin tube heat exchanger.

frontal velocity is 5 m/s. This plot represents the mid-plane between two adjacent fins. Fig. 9(a) shows that in the plain fin heat exchanger, the temperature of the wake region is significantly higher than that of the free-stream air flowing outside. This indicates that the free-stream air and the air in the wake region do not mix well, which is caused by the swirling characteristic of the wake as shown in the velocity vector plot of Fig. 5. When the DWVG are mounted on the plain fin, however, this high temperature region is reduced, as previously mentioned and shown in Fig. 9(b). The contour pattern of the air temperature distribution is quite similar to the velocity vector plot shown in Fig. 5. The similarity is because the air temperature is directly associated with convective heat transfer, which is controlled by the air flow itself. Early research proved that the convective heat transfer is a function of Reynolds number (Re) and Prandtl number (Pr), which explains the greater uniformity of the air temperature distribution of the DWVG fin heat exchanger in Fig. 10(b), compared with that of the plain fin heat exchanger. Fig. 11 provides a clear illustration through the plot of the temperature and velocity variation along the central line and across the second row of the tube. Fig. 11 shows that the DWVG causes a flatter temperature and velocity profiles at the rear of the heat transfer tube.

Fig. 10 shows the surface temperature distributions of the DWVG and plain fins. Both corners of the front end show low temperatures due to the higher heat transfer rate, which is caused by the higher velocity compared to the central region. As the location becomes closer to the tube, the fin surface temperature rises due to heat conduction through the fin itself. Moving away from the tube, the surface temperature declines and the air velocity rises. As noted above, the heat transfer performance in the wake region is poor. Consequently, the fin surface temperature appears high at the rear of the heat transfer tubes.

Fig. 11 shows that this high temperature region extends toward the rear end of the fin. The temperature levels around the second row tubes of the plain and DWVG fin are quite similar. However, those around the first row tubes are largely different due to the DWVG influence. The temperature level at the back of the first row tube of the DWVG fin is lower than that of the plain fin, because the DWVG reduced the wake region and facilitated air mixing, causing an enhanced heat transfer. Considering these observations, the DWVG can enhance convective heat transfer over a fin by reducing the wake region. Fundamental thermodynamic variables, the values of which are obtained via CFD analyses, are related with system pa-

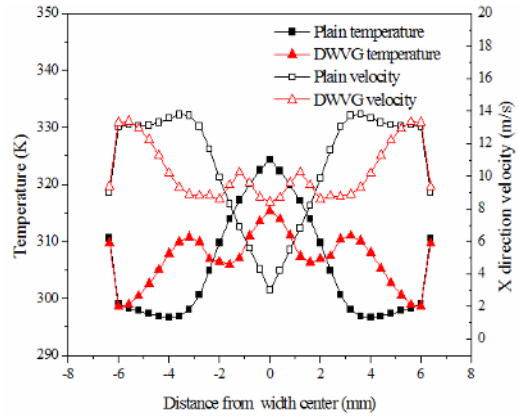

Fig. 11. Temperature and velocity of air along the line between the tubes of the 2nd row.

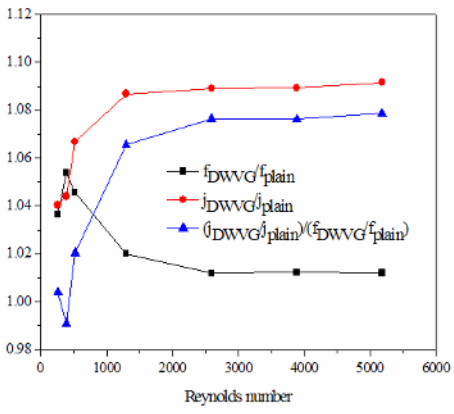

Fig. 13. Comparison of f-and j-factor ratios.

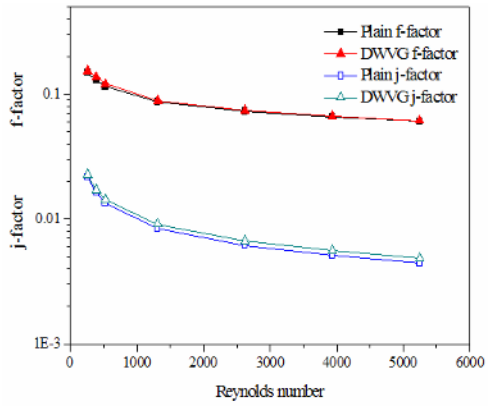

Fig. 12. Variation of f-and j-factors.

rameters such as the heat transfer and heat loss coefficients.

Fig. 12 shows the variation of the j- and f-factors with the frontal air velocity in a range of 0.5–20 m/s, and represented in terms of Reynolds number. For the conversion, the hydraulic diameter was used as the characteristic length scale, and is equivalent to double the fin pitch. The j-factor for the DWVG fin is larger than that of the plain fin over the whole range. Moreover, the f-factor variation showed an interesting trend. The f-factor of the DWVG fin is higher than that of the plain fin, but the difference diminishes with the increase in Reynolds number in a range of Re < 2500. Beyond Re = 2500, the f-factor of the DWVG fin becomes smaller than that of the plain fin. In a range of Re > 200, the j-factor of the DWVG fin remains larger than that of the plain fin. These results contradict the Reynolds analogy, which states that an enhanced surface wall has a larger f-factor, as delineated by Eq. (9). However, this analogy should not be expected to hold in the present situation; it is applicable to laminar and turbulent flows over a flat plate and a turbulent flow in a tube, but not during flow separation. If the tube and the wake region developed at the rear of the tube are not considered, the Reynolds analogy will become applicable. That is, the DWVG would generate longitudinal vortices and mix air to promote heat transfer. The DWVG would also obstruct flow to produce an additional form loss. In the present work, however, an additional effect occurred apart from the vortex generation: reduction of the wake region due to flow acceleration between the tube and the DWVG itself. This wave region reduction decreased the form loss. Therefore, the DWVG plays a dual role of increasing and reducing form loss due to the wake. As the Reynolds number increases, the effect of the form loss reduction becomes dominant over that of additional form loss. This explains how the f-factor of the DWVG fin becomes smaller than that of the plain fin.

Fig. 13 shows the ratio of the f- and j-factors of the DWVG fin compared with that of the plain fin. The f-factor ratio increases in a low Reynolds number range, but decreases as the Reynolds number increases. The j-factor ratio suddenly increases to 1.09 and do not change much thereafter. Another interesting plot is the j-factor ratio over the f-factor ratio. The Reynolds analogy states that an enhanced surface would have a value of '1'. The value obtained in previous fin design studies was frequently less than 1. However, Fig. 13 shows that the ratio of the present DWVG fin increases beyond '1' as the Reynolds number increases, implying that the present DWVG fin design will become more beneficial as the frontal air velocity increases.

Fig. 14 shows the variation of the area goodness factor with increasing Reynolds number. The area goodness factor is represented by heat transfer rate per frontal unit area, and is given as follows:

$$\frac{j}{f}=\frac{1}{A_f^2}\left(\frac{\mathrm{Pr}^{2/3}}{2\rho}\frac{NTU\times m^2}{\Delta P}\right). \tag{11}$$

A high area goodness factor means that a much smaller frontal area is necessary. In Fig. 14, the heat transfer performance is better than that of the plain fin heat exchanger when the Reynolds number is over 500, coinciding with the findings of Joardar and Jacobi [9].

Fig. 15 shows the variation of volume goodness factor with increasing Reynolds number. The volume goodness factor is

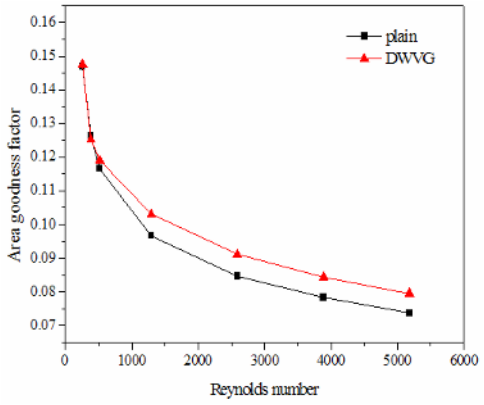

Fig. 14. Comparison of area goodness factor.

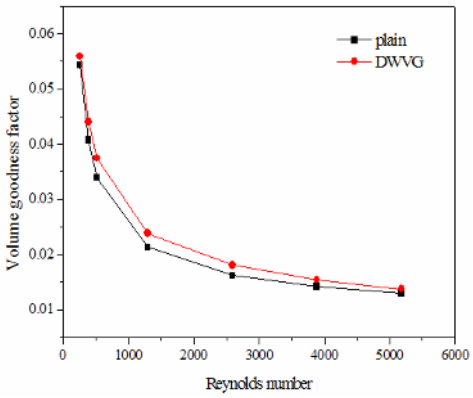

Fig. 15. Comparison of volume goodness factor.

represented by the heat transfer rate and pumping power per unit area, and is expressed as:

$$Volume\ goodness\ factor = \frac{St}{f^{1/3}}. \quad (12)$$

In Fig. 15, a high volume goodness factor needs a small volume to show the same performance in terms of heat transfer rate [18]. Using the DWVG causes a high volume goodness factor. Consequently, a smaller volume is required for the same pumping power.

4. Concluding remarks

In the past decade, numerous studies investigated the effect of vortex generators on the heat transfer of fins. While the vortex generators were consistently reported to enhance the heat transfer performance, the pressure loss measurements did not yield agreement. Despite significant research in this area, a lack of understanding remains on the mechanisms contributing to heat transfer augmentation and a limited increase in pressure loss. In the present work, the air flow and heat transfer in a fin-tube heat exchanger were analyzed using the CFD to obtain a better phenomenological understanding of the effects of the delta winglet vortex generator on fin performance. The flow acceleration between the delta winglet vortex generator and heat transfer tube delays the flow separation from the tube, which reduced the wake region at the rear of the tube. Thus, form loss is reduced and heat transfer is enhanced. Interestingly, the pressure loss of a fin with delta winglet vortex generators was even smaller than that of a plain fin with the enhanced heat transfer at high air velocity or Reynolds number. Comparing the results of the f- and j-factors, the performance of the DWVG fin improved as the Reynolds number increases in terms of enhanced heat transfer and reduced pressure drop penalty.

Acknowledgement

This work was supported by a 2-year research grant from the Pusan National University.

Nomenclature

a : Attack angle (°)
A_c : Area of fin collar (m^2)
A_{min} : Area of minimum air flow (m^2)
A_f : Area of frontal air flow (m^2)
A_{fin} : Area of fin (m^2)
b : Central angle (°)
C_f : Friction coefficient
C_p : Static pressure specific heat (kj/kg*K)
D : Tube diameter (m)
D_c : Characteristic length (m)
f : Fanning friction factor
f_v : Vortex shedding frequency (Hz)
g : Between tube and winglet gap (m)
h : Heat transfer rate (w/m^2*k)
H : Fin pitch (m)
j : Colburn j factor
k : Conductivity (W/m*K)
L : Length of heat exchanger (m)
P : Pressure (pa)
Q : Total heat flow (w)
t : Time (s)
t_{th} : Thickness (m)
T : Temperature (K)
T_c : Temperature of fin collar (K)
T_{in} : Inlet mean temperature (K)
T_{out} : Outlet mean temperature (K)
u : Velocity of x-axis (m/s)
U : Frontal fluid velocity (m/s)
v : Velocity of y-axis (m/s)
V_{in} : Frontal inlet velocity (m/s)
V_{max} : Maximum velocity (m/s)
W : Width of heat exchanger (m)
W_h : Winglet height (m)
W_l : Winglet length (m)
α : Thermal diffusivity (m^2/s)
μ : Dynamic viscosity ($N*s/m^2$)

ρ : Density (kg/m^3)
v : Kinetic viscosity (m^2/s)
Nu : Nusselt number
Pr : Prandtl number
Re : Reynolds number (ρ*V_{max}*D_h/ μ)
S : Strouhal number
St : Stanton number

References

[1] K. Chang and P. Long, An experimental study of the airside performance of slit fin-and-tube heat exchangers under dry and wet conditions, *International Journal of Air-Conditioning and Refrigeration,* 17 (1) (2009) 7-14.

[2] G. B. Schubauer and W. G. Spangenberg, Forced mixing in boundary layers, *Journal of Fluid Mechanics*, 8 (1960) 10-31.

[3] M. Fiebig, Vortices, generators and heat transfer, *Trans Institution of Chemical Engineers*, 76: Part A (1998).

[4] K. Torii, K. M. Kwak and K. Nishino, Heat transfer enhancement accompanying pressure-loss reduction with winglet-type vortex generators for fin-tube heat exchanger, *International Journal of Heat and Mass Transfer*, 45 (2002) 3795-3801.

[5] A. M. Jacobi and R. K. Shah, Heat transfer surface enhancement through the use of longitudinal vortices: A review of recent progress, *Experimental Thermal and Fluid Science*, 11 (1995) 295-309.

[6] M. Fiebig, A. Valencia and N. K. Mitra, Wing-type vortex generators for fin-and-tube heat exchangers, *Experimental Thermal and Fluid Science*, 7 (1993) 287-295.

[7] K. M. Kwak, K. Torii and K. Nishino, Heat transfer and pressure loss penalty for the number of tube rows of staggered finned-tube bundles with a single transverse row of winglets, *International Journal of Heat and Mass Transfer*, 46 (2003) 175-180.

[8] K. M. Kwak, K. Torii and K. Nishino, Simultaneous heat transfer enhancement and pressure loss reduction for finned-tube bundles with the first or two transverse rows of built-in winglets, *Experimental Thermal and Fluid Science*, 29 (2005) 625-632.

[9] A. Joardar and A. M. Jacobi, Heat transfer enhancement by winglet-type vortex generator arrays in compact plain-fin-and-tube heat exchanger, *International Journal of refrigeration*, 31 (2008) 87-97.

[10] C. B. Allison and B. B. Dally, Effect of a delta-winglet vortex pair on the performance of a tube-fin heat exchanger, *International Journal of Heat and Mass Transfer*, 50 (2007) 5065-5072.

[11] J. Min and W. Xu, Numerical prediction of the performances of the fins with punched delta winglets and the louver fins and their comparison, *Journal of Enhanced Heat Transfer*, 12 (4) (2005) 357-371.

[12] B. R. Munson, D. F. Young and T. H. Okiishi, *Fundamentals of fluid mechanics*, 4th edition. Wiley (2002).

[13] CD-adapco, *Methodology manual*, STAR-CD (2006).

[14] F. P. Incropera, D. P. Dewitt, T. L. Bergman and A. S. Lavine, *Introduction to heat transfer*, 5th edition. Wiley (2007).

[15] S. Kakac, H. Liu, *Heat exchangers,* CRC Press (1998).

[16] K. J. Kim and P. A. Durbin, Observations of the frequencies in a sphere wake and drag increase by acoustic excitation. *Physics of Fluids*, 31 (1998) 3260-3265.

[17] C. C. Wang, K. Y. Chi and C. J. Chang, Heat transfer and friction characteristics of plain fin-and-tube heat exchangers, part Ⅱ: Correlation. *International Journal of Heat and Mass Transfer*, 43 (2000) 2693-2700.

[18] R. K. Shah and K. London, Laminar flow forced convection in ducts, Academic Press, 1978.

Seong Won Hwang received his Master's degree for Mechanical Engineering at the Pusan National University in 2010. He is currently a Ph.D. candidate. His research interests include heat exchanger performance tests and CFD analyses. He is currently working on heat exchangers with offset strip fins and vortex generators.

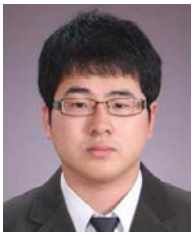

Dong Hwan Kim received his Master's degree for Mechanical Engineering at the Pusan National University in 2011. He works on heat transfer enhancement and its application to energy systems.

June Kee Min studied in KAIST and received his Ph.D. in 1999. He worked for LG Electronics and Samsung Electronics as a thermo-fluid engineer for over 10 years. He joined the Rolls-Royce Pusan National University Technology Center in 2008. His research interests mainly include CFD-based fluid flow and heat transfer problems, such as heat exchangers, HVAC&R, and the thermal management of power storage systems.

Ji Hwan Jeong received his Ph.D. from the KAIST in 1995. His post-doctoral research was conducted at the Technology Centre in Aerodynamics and Heat Transfer at Oxford University. After three years of research at the Korea Atomic Energy Research Institute, he joined the faculty of the School of Mechanical Engineering at Pusan National University. His research interests include multi-phase flow, nuclear safety, heat exchangers, heat pump, and computational fluid dynamics. He has also consulted for the nuclear and air conditioner industries.